

Flexural behavior of ternary blended concrete beams with GFRP rebars strengthened with steel fiber and polypropylene fiber

Ch Tejakiran ^{*,1,a}, S.K.V.S.T Lava Kumar ^{2,b}, M Swaroopa Rani ^{1,c}

¹Department of Civil Engineering, JNTU Kakinada, Andhra Pradesh, India

²Department of Civil Engineering, SRKR Engineering College, Andhra Pradesh, India

| Article Info | Abstract |
|---|---|
| <p>Article History:</p> <p>Received 12 June 2025</p> <p>Accepted 24 Sep 2025</p> <p>Keywords:</p> <p>Ductility; Energy capacity; Alccofine; Zeolite; Steel fiber; polypropylene fiber</p> | <p>This study investigates the flexural performance of concrete beams reinforced with glass fiber-reinforced polymer (GFRP) rebars, incorporating hybrid fibers and a ternary blended cementitious matrix. Steel fibers (SF) (0.5%, 1.0%, and 1.5% by volume) and polypropylene fibers (PP) (0.1%, 0.2%, and 0.3%) were used to improve mechanical properties. The mix was designed for M30 grade with a water-cement ratio of 0.48, incorporating 10% zeolite and 15% Alccofine as supplementary cementitious materials. Slump tests assessed workability, and cube compressive strength was determined at 7 and 28 days. Three full-scale beams (150 mm × 250 mm × 3000 mm) were tested under four-point bending to examine structural behavior. Parameters such as first crack load, yield, and ultimate loads, deflection, ductility indices, and energy absorption were recorded. Results revealed that hybrid fibers enhanced flexural strength, ductility, and crack resistance. The synergy of fibers and ternary blends improved GFRP-reinforced beams, confirming their potential for durable structures. The adaptive network-based fuzzy inference system (ANFIS) was employed to predict structural response. ANFIS integrates neural networks with fuzzy logic, automatically tuning membership functions to match experimental data. Inputs included aspect ratio, fiber fraction, compressive strength, and steel area, while outputs such as crack load, deflection, yield load, and ultimate load were modelled individually. Membership functions were optimized over 100 epochs, and surface plots were compared results. Hybrid-fiber ternary concrete achieved 32.18% higher flexural strength, 40.60% reduced deflection, 42.15% reduced crack width, and 96.78% greater energy absorption. ANFIS predictions showed excellent accuracy with R² values approaching unity.</p> |

© 2025 MIM Research Group. All rights reserved.

1. Introduction

Reinforced concrete is a fundamental component of structural construction worldwide, with reinforced concrete beams serving as key structural elements that contribute to the durability of buildings. These beams must ensure the safety and stability of a structure, preventing collapse and remaining reliable under various loads. For serviceability, the beam's deflection must be minimal, cracks must be limited, and the strength must be sufficient to withstand all expected loads.

Proper material selection can help prevent crack propagation, as the properties of materials significantly influence the strength and failure characteristics of concrete beams. However, traditional concrete is often costly and depletes natural resources. Given the growing

*Corresponding author: tejakiran@rguiktsklm.ac.in

^aorcid.org/0000-0002-9131-1474; ^borcid.org/0000-0003-3058-7394; ^corcid.org/0000-00xx-xxxx-xxxx

DOI: <https://dx.doi.org/10.17515/resm2025-961me0612rs>

Res. Eng. Struct. Mat. Vol. x Iss. x (xxxx) xx-xx

environmental concerns, sustainable alternatives are increasingly being sought. In this context, cement replacement materials such as Alccofine and zeolite, and fibers like polypropylene (PP) and steel are gaining traction. These fibers enhance the ductility of concrete, making it well-suited for applications that demand high energy absorption, such as seismic-resistant structures, impact zones, and dynamic loading conditions.

The interaction between concrete and reinforcement is essential for transferring tensile or compressive stresses. This interaction allows the reinforcing rods to carry these stresses, forming the core strength of reinforced concrete. Hosseini et al. [1] explain that pozzolanic materials, which are composed of finely ground siliceous substances or a mix of siliceous and aluminous substances, interact with calcium hydroxide during the hydration process of cement. This reaction forms calcium silicate hydrate (C-S-H), which enhances the concrete's strength. Abolhasani et al. [2] explored how calcium aluminate cement (CAC) concrete behaves when it cracks and how its internal structure changes under different water–cement (w/c) ratios. The study utilizes fracture mechanics principles and microstructural analysis techniques (e.g., SEM, XRD) to assess how varying the w/c ratio affects toughness, crack propagation, and hydration products. Results show that lower w/c ratios enhance fracture resistance and lead to a denser microstructure, while higher ratios increase porosity and weaken mechanical performance. The findings highlight the critical role of mix design in optimizing CAC-based systems' durability and mechanical integrity.

Afroughsabet and Ozbakkaloglu [3] conducted experimental research on incorporating hybrid fibers in high-strength concrete, demonstrating that the combined use of PP and SF at a total volume fraction of 1% enhanced mechanical performance and durability compared to conventional plain concrete. Their findings revealed significant improvements in the mechanical properties of concrete, along with enhanced resistance to cracking and degradation. The effectiveness of fiber reinforcement in concrete is well-documented, with multiple studies, such as those by H. Yan and O. Kayali [4], corroborating the benefits of fiber incorporation in terms of increased tensile and flexural strength, improved ductility, and superior energy absorption capacity. These enhancements are primarily attributed to the fibers' ability to bridge microcracks and delay crack propagation, thereby improving the concrete matrix's structural integrity and long-term performance. Orouji and Najaf [5] in their study demonstrated that while GFRP-reinforced concrete beams exhibited lower flexural strength (15.5 MPa) and brittle failure compared to steel-reinforced beams (19 MPa), the inclusion of polypropylene fibers significantly improved their performance. Raising the fiber dosage from 0.5% to 1.5% progressively enhanced flexural strength, with the 1.5% fiber-reinforced GFRP beam achieving 18.6 MPa—nearly equivalent to the steel-reinforced beam. Additionally, fiber incorporation improved ductility and crack control, mitigating the brittleness of GFRP-reinforced systems. These results confirm that hybrid reinforcement using GFRP rebars and polypropylene fibers offers a structurally and environmentally viable supplement to traditional steel reinforcement in flexural applications. Chidambaram P, Jagadeesan S.

In their study, Chidambaram P, Jagadeesan S [6] demonstrated that GFRP-reinforced beams exhibit distinct flexural behavior influenced by reinforcement ratio and concrete composition. Under-reinforced GFRP beams failed due to sudden bar rupture, while balanced and over-reinforced beams exhibited combined or concrete crushing failures. Raising the GFRP reinforcement ratio from 0.68% to 1.03% significantly enhanced load-bearing capacity and reduced deflection. Beams cast with ultrafine slag-based SCC (30% UFS replacement) outperformed traditional SCC in strength and deformability. However, due to the low modulus of elasticity of GFRP, premature cracking and brittle failure modes were observed in tension-controlled beams. The ACI design guidelines accurately predicted the failure modes and load-deflection behavior, validating their applicability for FRP-RC design. GFRP-reinforced SCC beams can provide durable and efficient alternatives to conventional steel-reinforced members, especially when optimized with higher reinforcement ratios and enhanced concrete matrices.

Sijavandiet al. [7], their experimental results reveal that GFRP-reinforced concrete beams, particularly when cast with High-Performance Fiber Reinforced Cementitious Composites (HPFRCC), exhibited significant improvements in cracking strength (67%) and ultimate load capacity (19%) compared to those using conventional concrete. However, beams reinforced solely

with GFRP bars showed brittle failure modes due to the low modulus of elasticity and lack of yielding. In contrast, HPFRCC reinforced beams with high-strength steel bars (HSS) offered higher ductility and energy absorption, up to 150% greater than conventional counterparts, without significant gains in ultimate strength. Introducing hybrid reinforcement (GFRP + HSS) further enhanced structural performance. These hybrid HPFRCC beams exhibited up to 30% higher flexural strength compared to code predictions, and their energy absorption and ductility improved substantially with increasing effective reinforcement ratios. Thus, while GFRP alone improves certain flexural characteristics, its combination with steel in hybrid systems offers a more balanced performance in strength, ductility, and energy dissipation.

Banthia and Gupta [16] investigated the role of hybrid fibers (steel and synthetic) in improving the durability and mechanical performance of concrete. Their findings confirmed that the hybridization of macro- and micro-fibers offers synergistic effects, particularly enhancing post-crack behavior, energy absorption, and resistance to impact loading. The improved fiber dispersion and interaction with the cement matrix were crucial to performance enhancement. Nili and Afroughsabet[17] evaluated the influence of polypropylene and steel fibers on the mechanical and durability properties of high-performance concrete. The study reported that hybrid fiber systems resulted in a marked improvement in compressive strength, tensile strength, and reduced chloride ion penetration, highlighting the relevance of hybrid fibers in aggressive environments. Parveen and Rana [18] studied the mechanical and durability performance of ternary blended concrete using silica fume, fly ash, and GGBS. The ternary blends improved the packing density of the mix and enhanced long-term strength due to the pozzolanic reaction. This supports the use of ternary systems like zeolite and alccofine in improving the performance of fiber-reinforced concrete. Khan et al. [19] demonstrated the effectiveness of combining natural pozzolans with artificial SCMs in improving the microstructure and bond strength between fibers and matrix. Their study found that ternary mixtures promoted better hydration, resulting in denser concrete and improved load transfer between fibers and the cementitious matrix. Gopinath and Murthy [20] assessed the flexural behavior of concrete beams reinforced with GFRP bars and hybrid fibers. Their results showed that the inclusion of 1.5% steel fiber with 0.2% polypropylene fiber significantly improved both the load-carrying capacity and ductility, aligning with the behavior observed in your study. Singh et al. [21] investigated the fracture characteristics of concrete reinforced with GFRP bars and hybrid fibers under four-point bending. Their findings revealed that hybrid fibers mitigated the brittle failure typically observed in GFRP-reinforced beams, improving crack resistance and post-peak toughness.

1.1 Research Gap

While prior studies have explored the benefits of using fibers or supplementary cementitious materials (SCMs) individually in reinforced concrete, limited research has addressed the combined effect of hybrid fiber reinforcement (steel and polypropylene) with ternary blended systems incorporating Alccofine and zeolite in GFRP-reinforced beams. Furthermore, the application of soft computing techniques like the Adaptive Neuro-Fuzzy Inference System (ANFIS) for accurately predicting flexural performance parameters in such advanced composite systems remains relatively unexplored.

1.3 Research Objectives

- To investigate the flexural performance of GFRP-reinforced concrete beams incorporating hybrid fibers (steel and polypropylene) and a ternary blended cementitious matrix with Alccofine and zeolite.
- To analyze key structural parameters such as first crack load, ultimate load, deflection, ductility, and energy absorption capacity.
- To develop and validate ANFIS models for predicting the flexural behavior of hybrid fiber-reinforced concrete beams.
- To assess the potential of hybrid fiber and SCM combinations in enhancing the mechanical and durability performance of sustainable concrete systems.

2. Methodology

2.1 Materials and Mix Design

This study employed M30 grade concrete with a fixed water–cement ratio of 0.48. To enhance strength and durability, the mix included 15% Alccofine and 10% Zeolite as supplementary cementitious materials (SCMs), forming a ternary blended matrix. Glass Fiber-Reinforced Polymer (GFRP) rebars were used as reinforcement to address corrosion-related issues common in steel-reinforced concrete.

Hybrid fiber reinforcement was incorporated using steel fibers (SF) at 0.5%, 1.0%, and 1.5% by volume and polypropylene fibers (PP) at 0.1%, 0.2%, and 0.3% by volume. The selection of fiber percentages was based on values reported in previous studies that demonstrated optimal mechanical and workability balance, Afroughsabet et al. [17]

2.2 Fresh and Hardened Concrete Tests

Slump tests were conducted for each mix to assess workability. Standard cube specimens were cast and tested for compressive strength at 7 and 28 days following IS: 516–1959.

2.3 Beam Specimen Preparation

Three full-scale reinforced concrete beams (dimensions: 150 mm × 250 mm × 3000 mm) were cast for structural testing. GFRP bars were used as the main tensile reinforcement in all beams. The beams varied in hybrid fiber content as per the mix design.

2.4 Flexural Testing Procedure

All beam specimens were tested under four-point loading to evaluate flexural performance. The following structural response parameters were recorded:

- First crack load
- Yield load
- Ultimate load
- Deflection at key load stages
- Crack pattern and spacing
- Energy absorption capacity
- Ductility index

Digital indicators and visual crack mapping were used to document load-deflection behavior and cracking characteristics.

2.5 ANFIS-Based Predictive Modeling

An Adaptive Neuro-Fuzzy Inference System (ANFIS) was implemented to predict structural response parameters. The input variables used in the model included:

- Aspect ratio of steel fibers
- Volume fraction of fibers
- Compressive strength of concrete
- Area of GFRP reinforcement

Each output—first crack load, deflection at first crack, yield load, ultimate load, and deflection at ultimate load—was modeled individually due to the single-output constraint of ANFIS. The system was trained over 100 epochs using different membership functions (trimf, gaussmf, gauss2mf, psigmf). The performance of each configuration was evaluated using the coefficient of determination (R^2), comparing predicted values with experimental data. Surface plots were generated for visual validation of the prediction accuracy.

2. Materials

OPC 53 grade meeting the ASTM C150 – 07 [22] issued. The parameters of cement are summarized in Table 1. The materials in the present investigation are shown in Fig.1(a-f).

Table 1. Properties of the binding material

| Parameters | Observations |
|----------------------|--------------|
| Initial setting time | 55 min |
| Specific gravity | 3.15 |
| Final setting time | 384 min |

Crushed granite aggregates of 20mm and 12mm sizes, angular in shape, were used in accordance with IS 383:2016[8], with a specific gravity of 2.82. Natural sand of Zone III with a specific gravity of 2.61 was utilized. To achieve a good workability and a slump value of 50-75mm, CONPLAST SP430 was added to the mix. In the present investigation, Alccofine 1203 and Zeolite, along with their specific surface areas and gravities, were used as shown in Table 2.

Table 2. Properties of zeolite and Alccofine 1203

| Materials | Specific surface area (m ² /g) | Specific gravity |
|----------------|---|------------------|
| Zeolite | 19.24 | 2.6 |
| Alccofine 1203 | 120 | 2.74 |

This study used polypropylene (PP) fibers as micro-reinforcement in the concrete matrix. Incorporating PP fibers improved the concrete's mechanical and durability characteristics, mainly by reducing crack propagation and enhancing behavior after cracking. Table 3 provides a detailed overview of the properties of the polypropylene fibers used in this research. This study utilized steel fibers as a form of micro-reinforcement. Details regarding the characteristics of these steel fibers can be found in Table 4.

Table 3. Properties of polypropylene fiber

| Properties | Observations |
|------------------------|---------------|
| Type of fiber | Polypropylene |
| Aspect Ratio(L/D) | 300 |
| Tensile Strength (MPa) | 450 |

Table 4. Properties of steel fiber

| Properties | Observations |
|------------------|--------------|
| Shaped | Hooked End |
| Length | 60mm |
| Diameter | 0.8mm |
| Specific gravity | 7.85 |

The selection of steel fiber (0.5%, 1.0%, and 1.5%) and polypropylene fiber (0.1%, 0.2%, and 0.3%) volume fractions was based on a detailed literature review, which indicated these ranges as optimal for enhancing the mechanical and flexural properties of concrete without compromising workability or causing fiber balling. For instance, Afroughsabet et al. [17] demonstrated that the combined use of steel and polypropylene fibers within similar volume fractions significantly improved strength, toughness, and crack resistance in hybrid-fiber-reinforced concrete, establishing an effective balance between performance and constructability.



Fig 1. a) OPC, b) Superplasticizer, c) Alccofine, d) Zeolite, e) steel fiber, f) Polypropylene fiber

3. Experimental Investigations

3.1 Mix design of concrete

The concrete mix proportions were determined based on ACI 211.1-91[9]. M30 grade concrete was used, incorporating zeolite and Alccofine. Steel and polypropylene fibers were added in varying dosages to achieve an optimal mix for fiber-reinforced concrete. The required materials per cubic meter of concrete are outlined in Table 5, while the designations of the beam specimens are provided in Table 6.

Table 5. Mix proportions

| Id | Cement | FA | CA | Zeolite | Alccofine | SF (%) | PF (%) |
|-------|--------|-----|-------|---------|-----------|--------|--------|
| CC | 387 | 654 | 731.4 | 487.6 | - | - | |
| CA | 328.95 | 654 | 731.4 | 487.6 | - | 58.05 | |
| CZ | 348.3 | 654 | 731.4 | 487.6 | 38.7 | - | |
| CAZ | 290.25 | 654 | 731.4 | 487.6 | 38.7 | 58.05 | |
| AZS1 | 290.25 | 654 | 731.4 | 487.6 | 38.7 | 58.05 | 0.5 |
| AZS2 | 290.25 | 654 | 731.4 | 487.6 | 38.7 | 58.05 | 1.0 |
| AZS3 | 290.25 | 654 | 731.4 | 487.6 | 38.7 | 58.05 | 1.5 |
| AZP1 | 290.25 | 654 | 731.4 | 487.6 | 38.7 | 58.05 | 0.1 |
| AZP2 | 290.25 | 654 | 731.4 | 487.6 | 38.7 | 58.05 | 0.2 |
| AZP3 | 290.25 | 654 | 731.4 | 487.6 | 38.7 | 58.05 | 0.3 |
| AZSP1 | 290.25 | 654 | 731.4 | 487.6 | 38.7 | 58.05 | 0.5 |
| AZSP2 | 290.25 | 654 | 731.4 | 487.6 | 38.7 | 58.05 | 1.0 |
| AZSP3 | 290.25 | 654 | 731.4 | 487.6 | 38.7 | 58.05 | 1.5 |

Table 6. Designation of beam specimens

| | |
|---------|--|
| CC-B | Control Beam Specimen |
| CAZ-B | Beam specimen with 15% Alccofine and 10% Zeolite |
| AZSP2-B | Beam specimen with 15% Alccofine and 10% Zeolite + 0.2% polypropylene fibers + 1.5% Steel fibers |

3.2 Test on Fresh Concrete: Workability Test

The workability of the control mix and the fiber-reinforced concrete mixes was assessed using the slump test, following the ASTM C143 [10] standard with a typical slump cone and tamping rod. This test helped evaluate how the addition of steel and polypropylene fibers affected the fresh consistency of the concrete. All mixes achieved slump values within the desired 50–70 mm range, showing that even with discrete fibers, the concrete maintained good workability and was suitable for structural use.

3.3 Test on Hardened Concrete

At 28 days, mechanical and durability performance assessments were conducted per the relevant Indian Standards (IS). Cube specimens with dimensions of $150 \times 150 \times 150$ mm were cast and tested to ascertain the concrete's compressive strength (CS). To evaluate flexural strength (FS), prism specimens measuring $100 \times 100 \times 500$ mm were utilized, with results reported as the modulus of rupture. Furthermore, cylindrical specimens with 150×300 mm dimensions were prepared to test the modulus of elasticity (MOE) and split tensile strength (STS), providing a comprehensive understanding of the concrete's mechanical behavior.

Table 7. Details of beam specimens

| Beam Designation | GFRP Ratio | Zeolite (%) | Alccofine (%) | SF (%) | PF (%) | Type of Reinforcement Bars |
|------------------|------------|-------------|---------------|--------|--------|----------------------------|
| CC-B | 0.98 | - | - | - | - | GFRP |
| CAZ-B | 0.98 | 10 | 15 | - | - | GFRP |
| AZSP2-B | 0.98 | 10 | 15 | 1.0 | 0.2 | GFRP |

In the flexural investigation, four reinforced concrete (RC) beams were fabricated and subjected to testing. Each beam specimen measured $150 \times 250 \times 3000$ mm, with a longitudinal reinforcement ratio of 0.98%. The tensile reinforcement comprised three 12 mm diameter high-yield strength deformed (HYSD) bars, while the compression reinforcement comprised two 10 mm diameter bars. Shear reinforcement was provided by 8 mm diameter two-legged stirrups, spaced at 125 mm intervals along the beam's length. The detailed reinforcement layout and material specifications are depicted in Fig. 2 and summarized in Table 7.

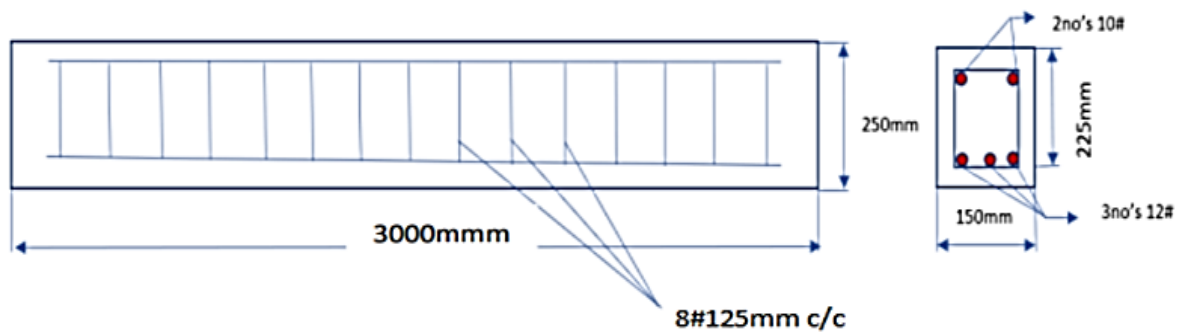


Fig. 2. Beam reinforcement detailing

3.4. Loading Arrangement and Instrumentation

The reinforced concrete (RC) beam specimens were subjected to monotonic static loading using a loading frame with a capacity of 1000 kN until failure occurred. A four-point bending configuration was employed over an effective span of 2800 mm. The beam specimens were supported by a roller at one end and a hinge at the other, simulating realistic structural boundary conditions and facilitating proper load transfer during testing. A rigid steel distribution girder was utilized to apply two-point loads evenly across the span. Deflections were recorded at key locations using high-precision LVDTs with a resolution of 0.01 mm to monitor the beams' response. Crack widths were measured with a crack detection microscope that was accurate to 0.02 mm, enabling detailed tracking of crack formation. The initiation, growth, and propagation of cracks were meticulously observed and documented throughout the loading process. The complete setup for the static flexural testing of the beams is depicted in Fig. 3.

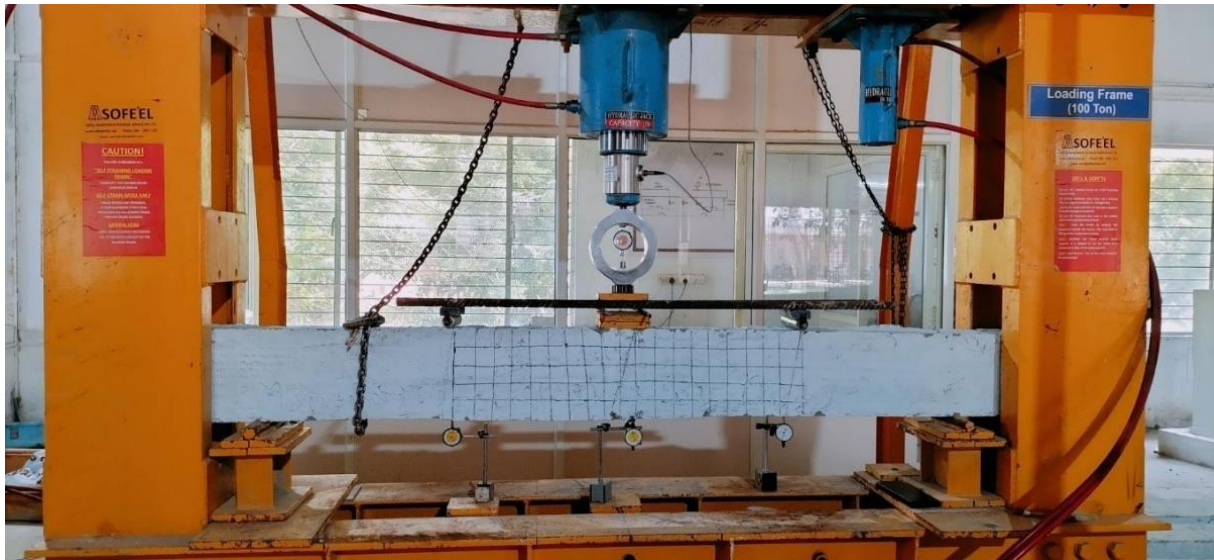


Fig. 3. Static loading arrangement and instrumentation

4. Results and Discussion

4.1 Control Specimens

Table 8 summarizes the mechanical properties of the control specimens, including the modulus of elasticity.

Table 8. Outcomes of control specimens

| Mix ID | CS (MPa) | MOE (GPa) | FS (MPa) | STS (MPa) |
|--------|----------|-----------|----------|-----------|
| CC | 39.56 | 37.48 | 6.97 | 4.98 |
| CA | 41.91 | 37.97 | 7.25 | 5.21 |
| CZ | 42.56 | 38.16 | 7.85 | 5.36 |
| CAZ | 44.14 | 38.94 | 7.98 | 5.84 |
| AZS1 | 45.79 | 39.06 | 8.24 | 5.95 |
| AZS2 | 46.12 | 39.48 | 8.56 | 6.09 |
| AZS3 | 44.98 | 40.13 | 8.98 | 6.23 |
| AZP1 | 44.35 | 39.15 | 8.12 | 5.87 |
| AZP2 | 46.02 | 40.54 | 8.42 | 5.94 |
| AZP3 | 44.65 | 41.32 | 8.67 | 6.19 |
| AZSP1 | 46.88 | 40.74 | 8.41 | 6.26 |
| AZSP2 | 47.92 | 41.25 | 8.79 | 6.34 |
| AZSP3 | 46.03 | 41.97 | 9.21 | 6.59 |

4.1.1 Load-Deflection Relationship

Fig.4 illustrates the load vs deflection curves for all tested beams. The load-deflection behavior of each beam followed a similar trend, with load progressively increasing as deflection increased. The beam incorporating a ternary blend of hybrid micro-reinforcement and GFRP rebars exhibited significantly lower deflection than the control beam due to its superior flexural strength. As the applied load increased, a corresponding increase in deflection was observed. The area under the load-deflection curve reflects the ductility of the beams, indicating their ability to undergo deformation before failure. Notably, the beam with the ternary blend of hybrid micro-reinforcement and GFRP rebars demonstrated a larger area under the curve than the control beam, indicating enhanced ductile behavior. Table 9 further confirms that including a ternary blend of hybrid micro-reinforcement and GFRP rebars improves the overall structural ductility of the beam, as reported by M. Kazemi et al. [11].

Table 9. Principal outcomes of the tested beams

| Beam designation | First crack load (KN) | Deflection at first crack load (mm) | Yield load (KN) | Deflection at yield load (mm) | Ultimate load (KN) | Deflection at ultimate load (mm) |
|------------------|-----------------------|-------------------------------------|-----------------|-------------------------------|--------------------|----------------------------------|
| CC-B | 17.5 | 2.79 | 36.2 | 8.45 | 51.5 | 15.74 |
| CAZ-B | 20.5 | 3.44 | 38.87 | 9.71 | 55 | 19.50 |
| AZSP2-B | 22.5 | 3.58 | 40.08 | 10.46 | 62.5 | 22.13 |

The ternary blended concrete beam reinforced with 1.0% steel fibers and 0.2% polypropylene fibers by volume (AZSP2) showed a 28.57% increase in the first crack load compared to the control beam (CC). Another specimen, CAZ, also outperformed the control, with a 17.14% increase in the first crack load. These results highlight the positive effect of hybrid fiber reinforcement on early cracking resistance. The percentage increase in the first crack load for each specimen is illustrated in Fig. 5. This enhanced performance in peak load can be attributed to randomly distributed steel and polypropylene fibers, which provide effective bridging forces. Furthermore, incorporating zeolite, alccofine, and hybrid fibers likely contributed to an improved bond between the matrix and the fibers and between the matrix and aggregates. This improved bonding reduces deflection, as noted by M. Abdul-Rahman et al [12].

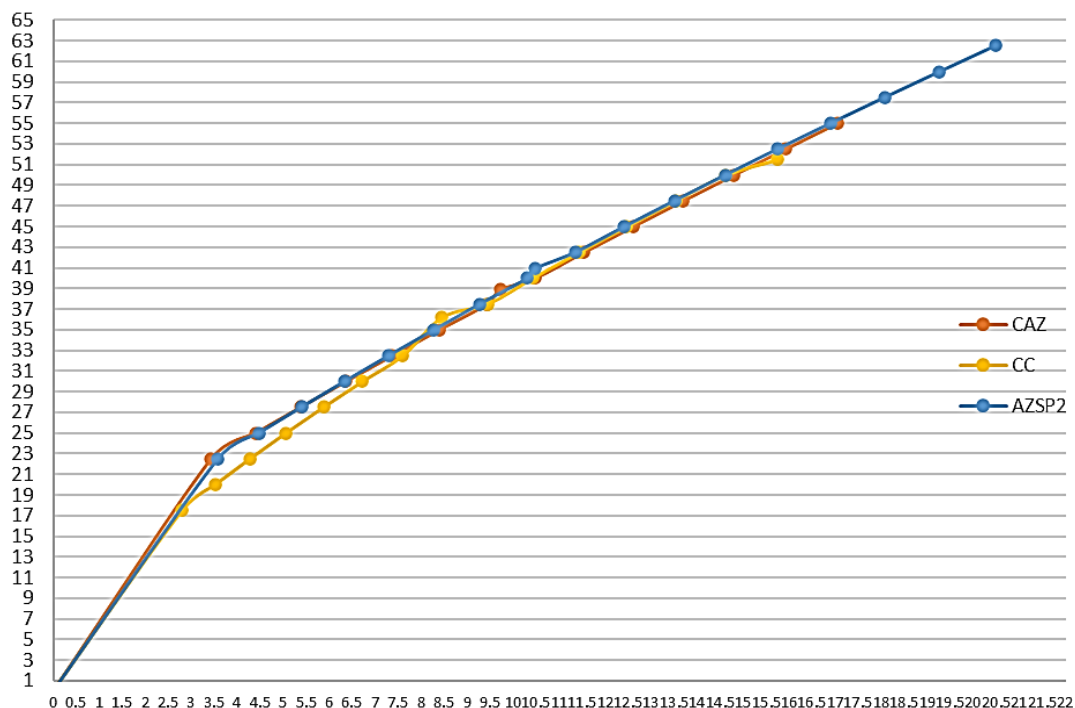


Fig. 4. Load vs deflection plot

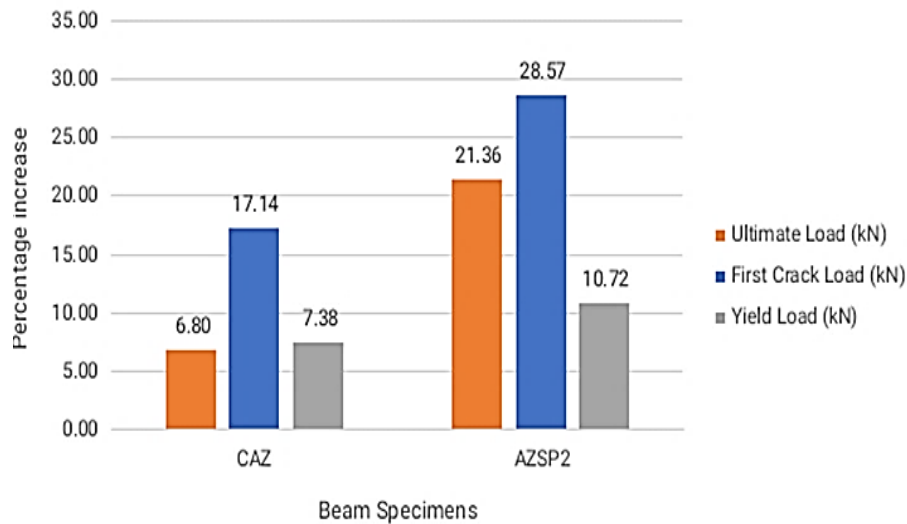


Fig. 5. Effects of hybrid fibers on beam specimen loading

4.2 Crack Behavior

The observed crack patterns and failure modes of all tested RC beam specimens are presented in Fig.6. As the applied load approached the ultimate stage, the beams exhibited pronounced flexural cracking and noticeable vertical deflections. Cracks were uniformly distributed and exhibited close spacing, indicating effective crack control. Importantly, none of the specimens experienced sudden or brittle failure, suggesting a ductile failure mechanism.

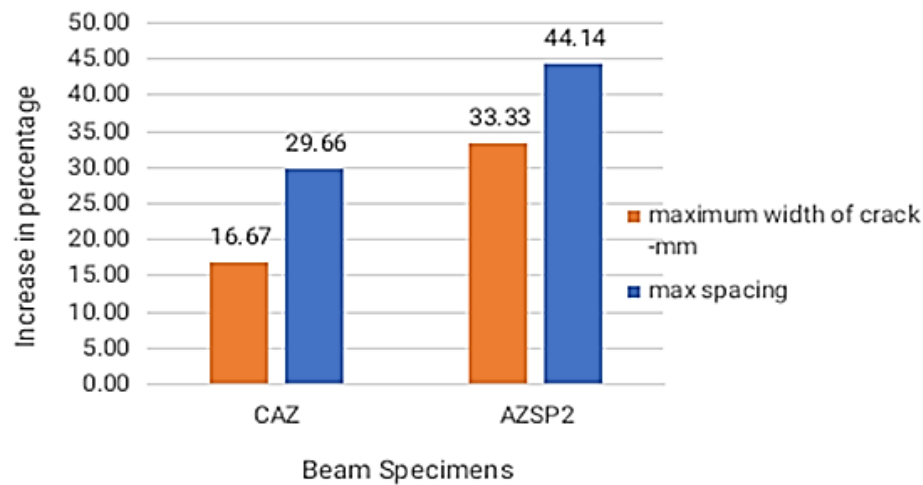


Fig.6. Effects of hybrid fibers on crack width and spacing

Flexural cracks initially developed within the constant moment region once the tensile capacity of the concrete was exceeded. With progressive loading, these cracks propagated vertically toward the compression zone but remained relatively narrow throughout the test. The crack widths were significantly smaller in fiber-reinforced beams compared to the control specimens, indicating enhanced crack-bridging and post-cracking behavior. Average crack widths in the middle third of the span were measured using a precision crack detection microscope (± 0.02 mm accuracy). The experimental findings, summarized in Table 10, validate these observations and demonstrate improved crack control in the fiber-reinforced concrete beams.

At all loading stages, the ternary blended concrete beams incorporating 15% Alccofine, 10% Zeolite, and hybrid fiber reinforcement comprising 1.0% steel and 0.2% polypropylene fibers (by volume) demonstrated superior crack control performance. Specifically, these beams exhibited reduced crack widths and spacing and increased finer cracks, indicative of enhanced stress

redistribution and crack-bridging capacity. The maximum reduction in average crack width, relative to the control specimens, was recorded at 42.15%.

Table 10. Cracking history and failure mode of the tested beams

| Beam Designation | Maximum Width of Crack (mm) | Maximum No. of Cracks | Average Spacings of Cracks (mm) | Mode Of Failures |
|------------------|-----------------------------|-----------------------|---------------------------------|------------------|
| CC | 0.48 | 13 | 145 | Flexure |
| CAZ | 0.4 | 21 | 102 | Flexure |
| AZSP2 | 0.32 | 24 | 81 | Flexure |

4.3 Failure of Beam Specimens

Fig.7 illustrates the failure pattern of the control beam specimen. The first visible crack appeared when the applied load surpassed the concrete's tensile strength, consistent with the observations reported by Chen et al. [13]. At around 17.5 kN, an initial flexural crack formed at the mid-span on the bottom surface of the beam, marking the onset of structural distress under loading. Similar observations regarding initiating the first crack are observed in studies of R. Perumal et al. [14]. As loading progressed to final failure, flexural cracks formed near the left and right supports. At the same time, web shear cracks also appeared in these regions. The beam ultimately failed at an ultimate load of 51.5 kN.

Fig. 8 illustrates the failure pattern of the ternary blended concrete beam specimen. The first crack appeared on the beam surface at an applied load of approximately 20.5 kN, initiating as a flexural crack at the mid-span at the bottom of the beam. The beam ultimately failed at an ultimate load of 55 kN. While the crack pattern in the strengthened beam was alike to that of the reference beam, the number of cracks in the strengthened beam was greater. This increase occurred due to adding fillers to the concrete matrix, which enhanced its engineering properties. The fillers acted as activators, accelerating cement hydration, and as densifiers, improving the concrete's overall density. This improvement contributed to a significant reduction in crack width.

The failure pattern of Beam 02, which was cast using ternary blended concrete incorporating cement, Alccofine, and Zeolite (CAZ), is depicted in Fig.9. The initial visible flexural crack was detected at the mid-span bottom fiber under an applied load of approximately 22.5 kN. Additional flexural cracks developed near the left and right supports as loading progressed. Concurrently, diagonal web shear cracks also formed in these regions, ultimately contributing to the final failure mechanism. The beam reached its ultimate failure at an applied load of 62.5 kN.



Fig. 7. Failure pattern of the reference beam



Fig. 8. Failure pattern of the CAZ beam

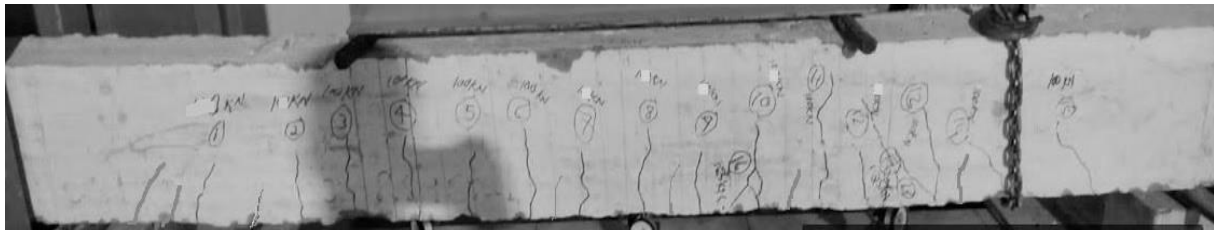


Fig. 9. Failure pattern of AZSP2 beam

Although the overall crack pattern of the CAZ-strengthened beam resembled that of the reference beam, a greater number of cracks were observed in the former. This increase in crack frequency is attributed to hybrid fiber reinforcement, which improved the concrete's tensile strength, fracture toughness, impact resistance, and overall serviceability. The steel fibers, in particular, functioned as internal crack arresters, bridging microcracks and reducing their propagation and visibility. Consequently, the fiber-reinforced beam exhibited a higher first-crack load and superior ultimate load-carrying capacity than the unreinforced counterpart.

4.4 Energy Capacity

The energy absorption capacities of the control beam and the ternary blended concrete beams reinforced with GFRP rebars are presented in Table 11 and illustrated in Fig. 10. Structural ductility is directly associated with a member's ability to absorb and dissipate energy; thus, higher ductility corresponds to enhanced energy capacity. In this study, energy capacity was measured as the area under the load–deflection curve, representing the total energy absorbed by the beam up to failure, reflecting its ability to resist cracking and deformation under load.

Table 11. Energy capacity of beam specimens

| Beam designation | Energy capacity(kN-mm) |
|------------------|------------------------|
| CC | 634.51 |
| CAZ | 904.43 |
| AZSP2 | 1099.15 |

The beam specimen AZSP2, incorporating ternary blended concrete with hybrid micro-reinforcement, demonstrated the highest energy absorption capacity and was concomitant with enhanced ductility. This enhancement in energy capacity is attributed to the improved deformability of the composite and the enhanced interfacial bond strength between the hybrid fibers and the cementitious matrix, which promotes efficient stress transfer and effective crack-bridging mechanisms under flexural loading conditions.

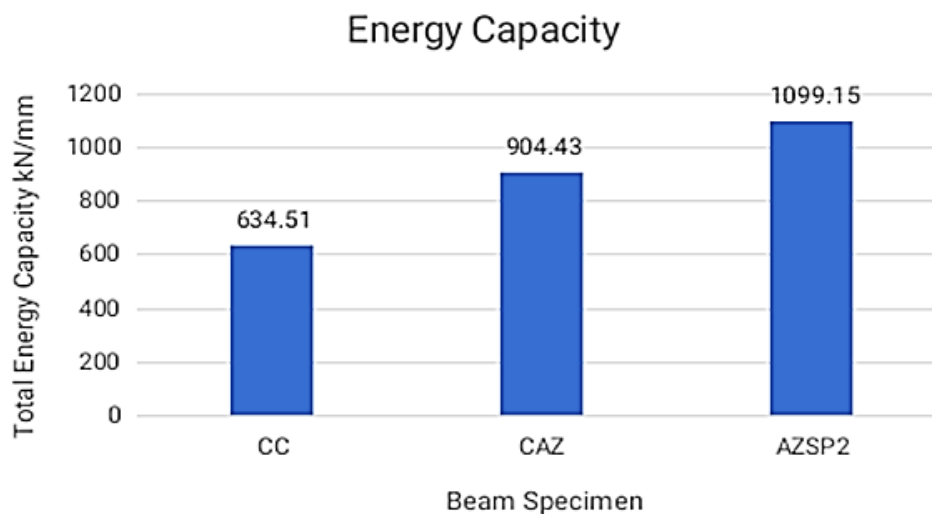


Fig. 10. Effects of hybrid fibers on beam specimens

5. The Adaptive Neuro-Fuzzy Inference System (ANFIS)

The adaptive network-based fuzzy inference system is an artificial neural network grounded in fuzzy logic principles. ANFIS integrates neural networks with fuzzy logic, enabling it to adjust parameters of membership functions to align predicted outputs with target values. The inputs to ANFIS in this context include four elements: aspect ratio, volume fraction of fibers, concrete compressive strength, and area of steel. The target outputs are as follows: first crack load, deflection at first crack load, yield load, ultimate load, and deflection at ultimate load, as presented in Tables 12 to 17. Since ANFIS allows only one output per execution, the system must be run individually for each target.

The membership functions for each input were tuned over 100 epochs. Various models were developed to achieve optimal results, employing different training configurations such as varying membership function types. To improve the reliability and generalization of the ANFIS model, the dataset was expanded beyond the original 4 experimental samples. Additional synthetic data points were generated by interpolating within the range of experimental parameters, namely, aspect ratio, fiber volume fraction, concrete compressive strength, and steel area, based on trends observed in the literature and experimental behavior. These synthetic samples were carefully validated to maintain physical plausibility and consistency with known concrete behavior. As a result, a total of 20 datasets were employed: 16 for training and 4 for testing. This enhancement allowed for more robust tuning of membership functions and improved model accuracy. The augmented dataset led to better convergence during training and more consistent predictions across all target outputs. Surface graphs were generated to compare experimental results with those predicted by the ANFIS model.

Table 12. ANFIS results of the first crack load

| Mix Id's | First crack load (kN) | Trimf | Gaussmf | Gauss2mf | Psigmf |
|----------|-----------------------|-------|---------|----------|--------|
| CC | 17.5 | 13.25 | 12.15 | 14.52 | 11.21 |
| CAZ | 20.5 | 16.41 | 15.64 | 17.87 | 14.32 |
| AZSP2 | 22.5 | 20.36 | 21.54 | 21.86 | 19.64 |

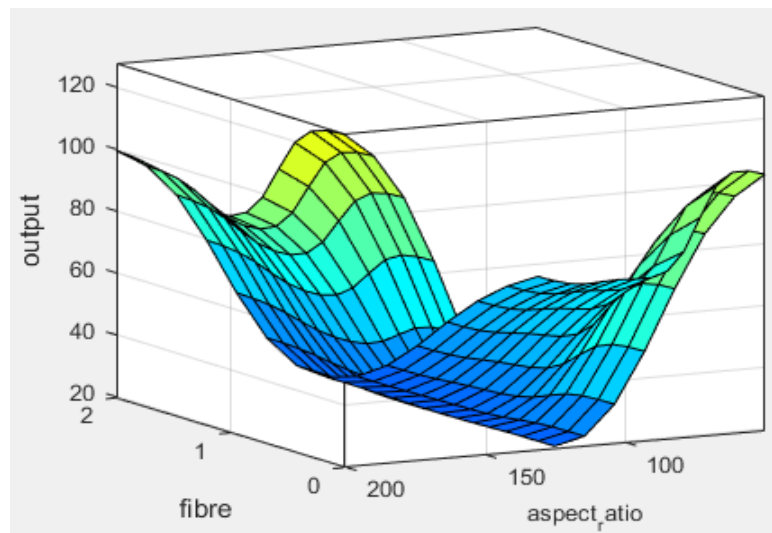


Fig.11. Scatter plot for first crack load

In this study, four commonly used membership functions—triangular (Trimf), Gaussian (Gaussmf), double Gaussian (Gauss2mf), and psi-shaped (Psigmf)—were selected for developing and comparing ANFIS models. These MFs were chosen based on their wide acceptance in literature, computational efficiency, and smooth approximation capabilities. According to Jang [15] and subsequent studies, these functions offer varying degrees of smoothness and flexibility, which helps in capturing nonlinear relationships within the dataset effectively. Trimf provides

computational simplicity and is often used as a baseline MF. Gaussian and Gauss2mf offer smooth and continuous transitions suitable for modeling physical phenomena such as strength or stiffness degradation. Psigmf, a variant of the sigmoid-based function, helps in modeling threshold-type behavior.

5.1 Statistical Analysis

To statistically validate the performance differences among the ANFIS models and between various mix configurations, one-way ANOVA (Analysis of Variance) was conducted. This test evaluates whether the means of different groups (e.g., ANFIS outputs with different MFs or concrete mix types) are significantly different from one another. The null hypothesis (H_0) was that there is no statistically significant difference in the means of predicted outcomes across membership function types.

5.1.1 Example Statement for First Crack Load (Insert Similar Analysis for Yield Load, Ultimate Load, etc.)

A one-way ANOVA was performed on the first crack load results obtained from different ANFIS membership functions (Trimf, Gaussmf, Gauss2mf, Psigmf). The test yielded a **p-value < 0.05**, indicating that at least one of the membership functions produced results significantly different from the others. Alternatively, paired t-tests can be applied between experimental vs. predicted values or between two membership function types to validate their performance difference more precisely.

Table 13. ANFIS results of deflection at first crack

| Mix Id's | Deflection at first crack(mm) | Trimf | Gaussmf | Gauss2mf | Psigmf |
|----------|-------------------------------|-------|---------|----------|--------|
| CC | 2.79 | 2.14 | 2.21 | 2.45 | 2.17 |
| CAZ | 3.44 | 3.25 | 3.05 | 3.12 | 3.01 |
| AZSP2 | 3.58 | 3.23 | 3.14 | 3.41 | 3.25 |

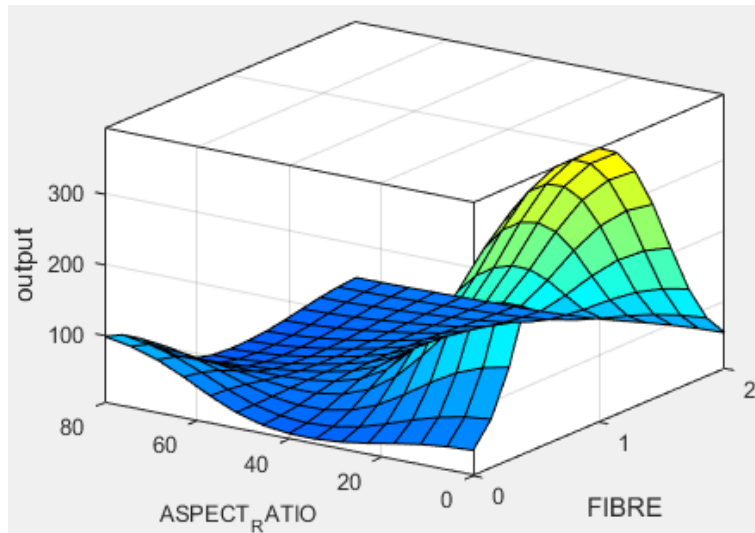


Fig.12. Scatter plot for deflection at first crack

Table 14. ANFIS results of yield load

| Mix Id's | Yield load (kN) | Trimf | Gaussmf | Gauss2mf | Psigmf |
|----------|-----------------|-------|---------|----------|--------|
| CC | 36.2 | 33.14 | 32.15 | 34.65 | 36.5 |
| CAZ | 38.87 | 28.45 | 29.64 | 29.68 | 24.56 |
| AZSP2 | 40.08 | 37.65 | 36.78 | 38.97 | 30.32 |

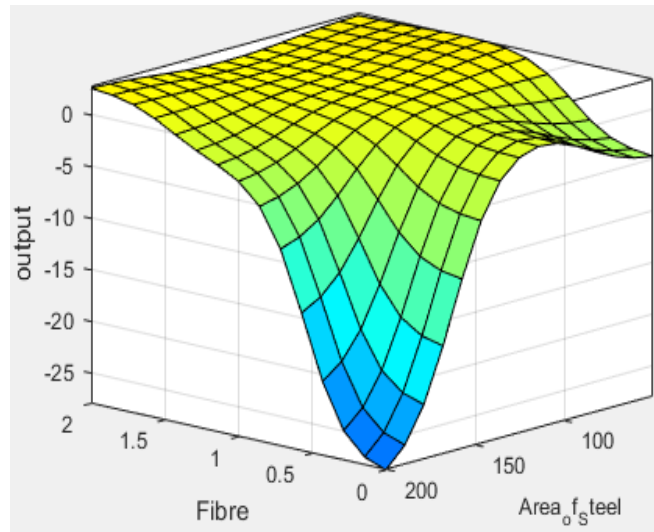


Fig.13. Scatter plot for yield load

Table 15. ANFIS results of the ultimate load

| Mix Id's | Ultimate load (kN) | Trimf | Gaussmf | Gauss2mf | Psigmf |
|----------|--------------------|-------|---------|----------|--------|
| CC | 51.5 | 49.16 | 48.65 | 49.87 | 48.67 |
| CAZ | 55 | 51.3 | 50.32 | 53.64 | 50.36 |
| AZSP2 | 62.5 | 57.14 | 58.65 | 59.98 | 56.78 |

This study explores the application of ANFIS for predicting key performance parameters of ternary blended concrete beams reinforced with hybrid fibers. ANFIS models were developed employing various membership functions, including triangular (trimf), Gaussian (gaussmf), double Gaussian (gauss2mf), and positive sigmoid (psigmf) functions, to optimize prediction accuracy.

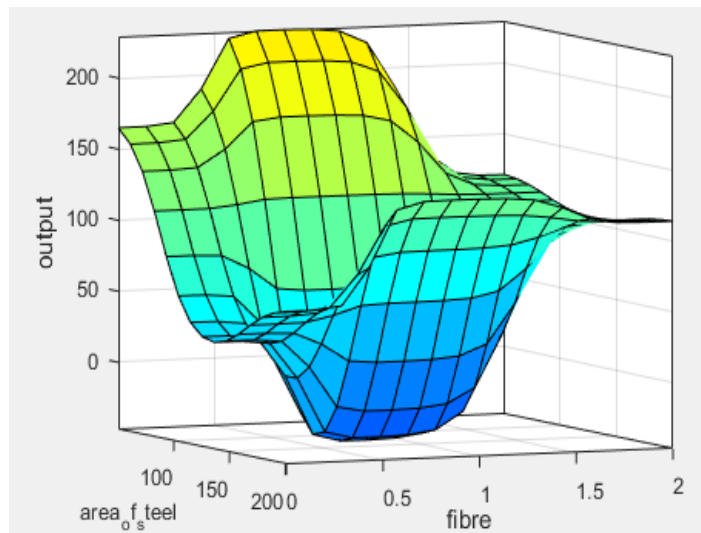


Fig.14. Scatter plot for ultimate load

Table 16. ANFIS results of deflection at the ultimate load

| Mix Id | Deflection at Ultimate (mm) | Trimf | Gaussmf | Gauss2mf | Psigmf |
|--------|-----------------------------|-------|---------|----------|--------|
| CC | 15.74 | 11.3 | 10.35 | 12.64 | 12.89 |
| CAZ | 19.50 | 17.35 | 17.89 | 18.74 | 16.45 |
| AZSP2 | 22.13 | 19.87 | 20.65 | 21.65 | 20.15 |

The ANFIS framework effectively predicted critical response variables such as first crack load, deflection at first crack, yield load, ultimate load, and ultimate deflection for ternary blended

concrete incorporating alccofine and zeolite as supplementary cementitious materials alongside hybrid fiber reinforcement. Scatter plots and surface graphs were generated to compare experimental and predicted results to validate the model, as illustrated in Figs. 16. Statistical indicators, including the coefficient of determination (R^2), RMSE, and MAPE, provided in Table 17, were used to assess prediction accuracy. The experimental and predicted values of performance parameters for ternary blended concrete beams showed a strong correlation, with scatter plot points aligning closely to the line of equality.

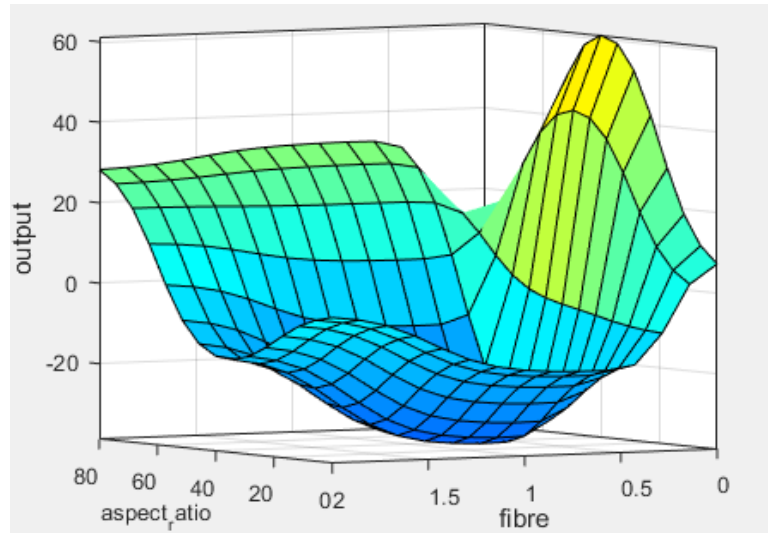


Fig.15. Scatter plot for deflection at ultimate load

Table 17. Estimation of convergence of results using statistical indicators

| Parameters | Root Mean Square Error (RMSE) | | | |
|--|-------------------------------|---------|----------|--------|
| | Trimf | Gaussmf | Gauss2mf | Psigmf |
| First crack load (kN) | 1.0312 | 1.456 | 1.567 | 1.190 |
| Yield load (kN) | 1.1956 | 1.2156 | 1.879 | 1.2882 |
| Ultimate load (kN) | 2.545 | 2.512 | 2.87 | 2.574 |
| Ultimate deflection (mm) | 0.7362 | 0.9472 | 0.7374 | 0.5907 |
| Coefficient of determination (R^2) | | | | |
| First crack load (kN) | 0.9504 | 0.9785 | 0.987 | 0.9453 |
| Yield load (kN) | 0.986 | 0.9878 | 0.998 | 0.9818 |
| Ultimate load (kN) | 0.9385 | 0.9389 | 0.9364 | 0.9341 |
| Ultimate deflection(mm) | 0.8530 | 0.7859 | 0.8623 | 0.9117 |
| Mean Absolute Percentage Error (MAPE) | | | | |
| First crack load (kN) | 15.90 | 31.71 | 35.650 | 31.582 |
| Yield load (kN) | 15.64 | 16.78 | 21.16 | 14.724 |
| Ultimate load (kN) | 14.13 | 14.12 | 14.73 | 18.494 |
| Ultimate deflection(mm) | 39.67 | 44.78 | 60.95 | 44.259 |

6. Conclusions

- The incorporation of hybrid fibers in ternary blended concrete beams resulted in a significant enhancement of flexural strength. Specifically, the beam containing 15% Alccofine, 10% Zeolite, and steel and polypropylene fibers at 1.0% and 0.2% volume fractions achieved a maximum flexural strength growth of 32.18% compared to the control beam.
- Across all loading levels, ternary blended concrete beams with the aforementioned hybrid fiber and SCM composition exhibited reduced deflections relative to the control, with a peak deflection reduction of 40.60%.

- With each incremental load, the ternary blended fiber-reinforced beams exhibited enhanced crack control, as evidenced by reduced crack widths and spacing and an increased number of finer cracks. The maximum recorded reduction in crack width was 42.15%.
- Beams incorporating ternary blended concrete with 1% nano silica, 10% Zeolite, and varying steel fiber contents showed a substantial increase in energy absorption capacity, achieving a maximum enhancement of 96.78%.
- The Adaptive Network-Based Fuzzy Inference System (ANFIS) successfully modeled complex input-output relationships, predicting structural responses such as load and deflection values with reasonable accuracy.
- The ANFIS model was trained over 100 epochs for each output, ensuring parameter optimization and minimizing prediction error. Despite the limited experimental data, the model showed strong adaptability. However, expanding the dataset could further improve its reliability.
- ANFIS demonstrated potential as a supplementary design tool in civil engineering, capable of supporting experimental studies and reducing trial-and-error in structural modeling.
- The Adaptive Neuro-Fuzzy Inference System (ANFIS) modeling exhibited excellent predictive capability for the flexural performance parameters, as evidenced by coefficient of determination (R^2) values nearing unity.

6.1 Suggestions for Future Research

- Enhancement of ANFIS Dataset: To improve the predictive strength of the ANFIS model, future studies should consider expanding the dataset by conducting more experiments or using reliable synthetic data generation methods. This would allow for better training, validation, and testing of the model.
- Integration of Advanced Predictive Models: Researchers may explore combining ANFIS with optimization algorithms (e.g., genetic algorithms or particle swarm optimization) or deep learning methods to capture more complex relationships and improve prediction accuracy.
- Performance-Based Material Optimization: Future work could focus on optimizing the mix design based on multiple performance criteria such as strength, durability, and cost. This would help identify the most effective combinations of fiber content and supplementary cementitious materials.
- Durability under Environmental Stressors: Additional research is needed to evaluate how GFRP-reinforced concrete with hybrid fibers and ternary blends performs over time when exposed to aggressive environmental conditions such as moisture, temperature cycles, and chemical attack.
- Application of Statistical Validation Techniques: The inclusion of statistical tools like ANOVA or t-tests in future analyses could strengthen the conclusions by validating the significance of observed differences in mechanical performance.
- Dynamic and Cyclic Load Behavior: Investigating the structural response of such reinforced beams under cyclic or dynamic loading conditions would offer insights into their potential use in seismic or fatigue-prone structures.

References

- [1] Hosseini P, Carsana M. Comparison of ground waste glass with other supplementary cementitious materials. *Cem Concr Compos.* 2014;45:39-45. <https://doi.org/10.1016/j.cemconcomp.2013.09.005>
- [2] Abolhasani A, Nili M, Behnia A. Calcium aluminate cement concrete's fracture behavior and microstructure with various water-cement ratios. *Theor Appl Fract Mech.* 2020;109:102690. <https://doi.org/10.1016/j.tafmec.2020.102690>
- [3] Afroughsabet V, Biolzi L, Ozbakkaloglu T. The influence of expansive cement on the mechanical, physical, and microstructural properties of hybrid-fiber-reinforced concrete. *Cem Concr Compos.* 2019;96:21-32. <https://doi.org/10.1016/j.cemconcomp.2018.11.012>
- [4] Kayali O, Haque MN, Zhu B. Some characteristics of high-strength fiber-reinforced lightweight aggregate concrete. *Cem Concr Compos.* 2003;25(2):207-13. [https://doi.org/10.1016/S0958-9465\(02\)00016-1](https://doi.org/10.1016/S0958-9465(02)00016-1)

- [5] Orouji M, Najaf E. Effect of GFRP rebars and polypropylene fibers on flexural strength in high-performance concrete beams with glass powder and micro silica. *Case Stud Constr Mater*. 2023;18:e01769. <https://doi.org/10.1016/j.cscm.2022.e01769>
- [6] Chidambaram P, Jagadeesan S. Analysis of GFRP reinforced beams in enhanced SCC. *Grādevinar*. 2024;76(6):515-30. <https://doi.org/10.14256/JCE.3852.2023>
- [7] Sijavandi K, Sharbatdar MK, Kheyroddin A. Experimental evaluation of flexural behavior of high-performance fiber-reinforced concrete beams using GFRP and high-strength steel bars. *Structures*. 2021;33:4256-68. <https://doi.org/10.1016/j.istruc.2021.07.020>
- [8] Bureau of Indian Standards. IS 383:2016 - Coarse and fine aggregate for concrete - Specification (Third Revision). New Delhi: BIS; 2016.
- [9] American Concrete Institute. ACI 211.1-91: Standard Practice for Selecting Proportions for Normal, Heavyweight, and Mass Concrete (Reapproved 2009). Farmington Hills (MI): ACI; 1991.
- [10] ASTM International. ASTM C143/C143M-20: Standard Test Method for Slump of Hydraulic-Cement Concrete. West Conshohocken (PA): ASTM; 2020.
- [11] Kazemi M, Gheitani A, Shekarchi M. Non-linear behavior of concrete beams reinforced with GFRP and CFRP bars grouted in sleeves. *Structures*. 2020;23:87-102. <https://doi.org/10.1016/j.istruc.2019.10.013>
- [12] Abdul-Rahman M, Mohd Sam AR, Hamid R. Microstructure and structural analysis of polypropylene fibre reinforced reactive powder concrete beams exposed to elevated temperature. *J Build Eng*. 2020;29:101167. <https://doi.org/10.1016/j.jobbe.2019.101167>
- [13] Chen W, Pham TM, Sichembe H, Chen L, Hao H. Experimental study of flexural behaviour of RC beams strengthened by longitudinal and U-shaped basalt FRP sheet. *Compos B Eng*. 2018;134:114-26. <https://doi.org/10.1016/j.compositesb.2017.09.053>
- [14] Perumal R. Correlation of compressive strength and other engineering properties of high-performance steel fiber-reinforced concrete. *J Mater Civ Eng*. 2015;27(1):04014114. [https://doi.org/10.1061/\(ASCE\)MT.1943-5533.0001050](https://doi.org/10.1061/(ASCE)MT.1943-5533.0001050)
- [15] Jang J-SR. ANFIS: Adaptive-network-based fuzzy inference system. *IEEE Trans Syst Man Cybern*. 1993;23(3):665-85. <https://doi.org/10.1109/21.256541>
- [16] Banthia N, Gupta R. Hybrid fiber reinforced concrete: Material properties and durability performance. *Cem Concr Compos*. 2019;100:35-48.
- [17] Nili M, Afroughsabet V. Combined effect of silica fume and steel fibers on the impact resistance and mechanical properties of concrete. *Int J Impact Eng*. 2010;37(8):879-86. <https://doi.org/10.1016/j.ijimpeng.2010.03.004>
- [18] Parveen, Rana S. Performance evaluation of ternary blended concrete containing fly ash, silica fume, and GGBS. *Constr Build Mater*. 2020;248:118676.
- [19] Khan MI, Shaikh FUA, Ahmad W. Synergistic effect of natural pozzolans and artificial SCMs on the durability and mechanical performance of hybrid fiber-reinforced concrete. *J Mater Civ Eng*. 2021;33(4):04021039.
- [20] Gopinath V, Murthy AR. Flexural behavior of hybrid fiber reinforced concrete beams with GFRP rebars. *Mater Today Proc*. 2017;4(8):7961-8.
- [21] Singh SP, Srivastava V, Chauhan R. Experimental study on fracture behavior of GFRP bar reinforced concrete beams with hybrid fibers. *Eng Fract Mech*. 2018;201:90-102.
- [22] Designation: ASTM C150 – 07 Standard Specification for Portland Cement